

# Space-Time $D$ -Block Codes via the Virtual MIMO Channel Representation

Ke Liu, *Student Member, IEEE*, and Akbar M. Sayeed, *Senior Member, IEEE*

**Abstract**—We apply the recently introduced virtual channel representation to the problem of space-time coding for correlated multiple-input multiple-output (MIMO) channels. The virtual channel representation clearly reveals the essential degrees of freedom in correlated MIMO channels and the corresponding statistical channel structure. Coding design criteria for general correlated channels are derived from pairwise error probability analysis, which reveal the effect of channel statistics and codeword properties on code performance. We focus on the  $K$ -diagonal model for correlated channels whose nonvanishing elements correspond to  $K$  diagonals of the virtual channel matrix. The  $K$ -diagonal model can be motivated by physical scattering considerations or as a low-dimensional approximation to the channel matrix that serves as a building block for general correlated channels. Space-time  $D$ -block codes that attain  $D$ -level diversity (related to  $K$ ) per receive dimension are constructed using the theory of space-time block codes. Compared with space-time block codes, identical performance but with significantly smaller delay and complexity can be achieved by matching space-time  $D$ -block codes to the  $K$ -diagonal channel structure. Our construction also facilitates a natural tradeoff between rate and diversity by decomposing the original channel into several parallel virtual  $K$ -diagonal subchannels. Simulation results demonstrate the excellent performance of the proposed techniques.

**Index Terms**—Orthogonal designs, space-time block codes, space-time coding, virtual channel representation.

## I. INTRODUCTION

RECENT studies indicate that antenna arrays hold great promise for bandwidth-efficient high speed wireless communication [1], [2]. Maximal exploitation of antenna arrays in wireless communication necessitates accurate yet tractable modeling of the multi-input multi-output (MIMO) channel coupling the transmitter and receiver. Most existing models belong to two extreme cases: 1) an idealistic statistical model that consists of independent identically distributed (i.i.d.) channel coefficients representing a rich scattering environment (see, e.g., [1]–[3]), and 2) parametric physical models that model the channel via signal propagation along multiple paths (see, e.g., [4]). To date, majority of coding works on antenna arrays (see, e.g., [1], [3]) have focused on the i.i.d. channel partly because of its mathematical tractability. These works have yielded many elegant results and precious insights. However, realistic

MIMO channels exhibit correlated fading due to clustered scattering that can substantially reduce the intrinsic diversity and degrees of freedom in the MIMO channel. Recent studies (see, e.g., [5]–[7]) have demonstrated that capacity of correlated channels can significantly deviate from that of i.i.d. channels. Moreover, channel correlation causes mismatch with code design criteria derived from the i.i.d. channel model, thereby resulting in performance degradation, severe in many cases, of existing space-time codes [8], [9]. Evidently, new space-time code designs that account for the interaction between channel characteristics and code properties are desirable both from theoretical and practical viewpoints. As one such attempt, a robust criterion on code design that is not channel-dependent was proposed in [10]. This approach is useful if channel characteristics are unknown. However, when information about channel structure/statistics is known, it should be exploited as it usually results in significantly improved performance. Lack of space-time coding techniques that exploit the structure of correlated MIMO channels is partly due to the lack of tractable channel models that characterize such structure.

In this paper, we attack the problem of space-time code design for correlated channels based on the recently introduced virtual channel representation for MIMO fading channels [5]. The virtual representation keeps the essence of physical modeling (without its complexity) as well as the tractability of the idealized statistical model. It yields a linear channel characterization in terms of fixed spatial basis functions (defined by fixed virtual angles) whose expansion coefficients form the virtual channel matrix. In clustered scattering environments, the virtual channel matrix can be decomposed into nonvanishing submatrices corresponding to different clusters. The nonvanishing elements of the virtual matrix are approximately uncorrelated under the assumption of uncorrelated physical scattering and thus characterize the essential degrees of freedom in the channel. Consequently, insights from the large body of coding work on i.i.d. channels can be applied to correlated channels in the virtual representation.

Our study focuses on a particular channel structure, the  $K$ -diagonal (virtual) channel, whose nonvanishing elements correspond to  $K$  nonvanishing diagonals of the virtual channel matrix. The  $K$ -diagonal model arises from physical scattering considerations to capture channel correlation and serves as a basic modeling unit for more general channel structures—the overall channel can be approximated by a concatenation of various  $K$ -diagonal subchannels. More importantly, the  $K$ -diagonal model provides a close and flexible approximation to channel capacity and diversity afforded by the overall channel [5]. In particular, small  $K$  represents high correlation (low diversity) and large  $K$  for low correlation (high diversity). Exploiting  $K$ -diagonal channel structure enables us to construct

Manuscript received November 22, 2002; revised January 14, 2003; accepted February 20, 2003. The editor coordinating the review of this paper and approving it for publication is M. Shafi. This work was supported in part by the National Science Foundation under Grant CCR-9875805 and in part by the Office of Naval Research under Grant N00014-01-1-0825.

The authors are with the Department of Electrical and Computer Engineering, University of Wisconsin-Madison, Madison, WI 53706 USA (e-mail: kliu@cae.wisc.edu; akbar@engr.wisc.edu).

Digital Object Identifier 10.1109/TWC.2004.827761

space-time  $D$ -block codes, based on space-time block codes [11], for  $K$ -diagonal channels ( $D$  is related to  $K$ ). Space-time  $D$ -block codes achieve full diversity with much smaller delay and complexity than that of space-time block codes. The design criteria, derived from pairwise error probability analysis, clearly reveal the role of channel characteristics on code performance. In particular, regardless of the channel correlation, the channel correlation matrix is approximately diagonal in the virtual representation, which greatly simplifies the code design.

The notion of virtual angle grouping is introduced to show that space-time  $D$ -block codes essentially partition the original virtual channel matrix into several classes with each class collectively contributing to one level of diversity. By choosing a suitable  $D$ , designers may reduce total level of diversity in exchange for smaller processing delay and complexity. A related important benefit of the virtual representation is that it naturally facilitates diversity-versus-rate tradeoff, which overcomes the rate deficiency associated with space-time block codes (and space-time  $D$ -block codes as well) [11]–[13] relative to high rate schemes such as spatial multiplexing (see, e.g., [1]). Applying the principle of combining array processing and space-time coding in [14], we propose a “divide-and-conquer” approach in Section V to decompose the original channel into several lower dimensional subchannels which can support multiple independent data streams simultaneously. However, interference among different subchannels in general may create a bottleneck in system performance. A simple iterative interference cancellation scheme is proposed to mitigate such interference. Numerical results presented in the paper show the impressive performance of the proposed techniques. Overall, the results of this paper demonstrate that the virtual channel representation provides an ideal framework for matching statistical channel characteristics to code properties for significantly improved performance.

We review the virtual channel representation and  $K$ -diagonal channel in the next section. Readers are referred to the original work [5] for more details. In Section III, an upper bound on pairwise error probability (PEP) of space-time codes that subsumes the classical results given in [3] is derived to obtain design criteria for general correlated channels. The PEP analysis motivates space-time  $D$ -block codes that are discussed in detail. In Section IV, space-time  $D$ -block codes are interpreted via virtual angle grouping. Section V discusses a simple framework for trading off rate for diversity. Concluding remarks are provided in Section VI.

The following notation is used throughout this paper.  $(\cdot)^\top$ ,  $(\cdot)^\dagger$ , and  $(\cdot)^*$  stand for transposition, conjugate transposition, and conjugation, respectively. Let  $\|\cdot\|$  and  $\|\cdot\|_F$  denote the Euclidean norm of a vector and the Frobenius norm of a matrix [15]. The  $n$ -dimensional real (complex) Gaussian distribution is denoted by  $(\mathbf{C})\mathcal{N}^n(\mathbf{m}, \mathbf{R})$  where  $\mathbf{m}$  and  $\mathbf{R}$  are the mean and covariance of the distribution, respectively. Let  $a_1, \dots, a_n$  be a sequence of independent  $\mathcal{N}^1(0, 0.5)$  random variables. Then,  $\sum_{i=1}^n a_i^2$  is chi-square distributed with  $n$  degree of freedom, denoted by  $\chi_n^2$ . The  $n \times n$  identity matrix is denoted by  $\mathbf{I}_n$ . The Kronecker product  $\mathbf{A} \otimes \mathbf{B}$  between matrices  $\mathbf{A}$  and  $\mathbf{B}$  is defined by  $\mathbf{A} \otimes \mathbf{B} = (a_{ij}\mathbf{B})$ . Let  $\mathbf{A} = (\mathbf{a}_1, \dots, \mathbf{a}_n)$  where  $\mathbf{a}_i$ ,  $1 \leq i \leq n$ , is the  $n$ -th column of  $\mathbf{A}$ . Denote by  $\text{vec}(\mathbf{A})$  the column vector obtained by stacking columns of  $\mathbf{A}$ .

## II. VIRTUAL CHANNEL REPRESENTATION AND $K$ -DIAGONAL CHANNELS

Consider a multiple antenna system with  $N$  transmit and  $M$  receive elements. The  $M$ -dimensional received signal  $\mathbf{r}$  and the  $N$ -dimensional transmitted signal  $\mathbf{s}$  are related as

$$\mathbf{r} = \mathbf{H}_c \mathbf{s} + \mathbf{w} \quad (1)$$

where  $\mathbf{w}$  is noise and  $\mathbf{H}_c$  denotes the channel matrix coupling pairs of transmit and receive elements. The statistics of  $\mathbf{H}_c$  determine channel capacity and diversity. Most capacity calculations and space-time code design assume  $\mathbf{H}_c$  to consist of i.i.d. Gaussian random variables—an idealized, rich scattering environment (see, e.g., [1], [2]). Generally speaking, the statistics of  $\mathbf{H}_c$  are dictated by factors such as physical scattering characteristics, antenna geometry and operating frequencies, etc. Realistic propagation environments can be modeled as a superposition of scattering clusters (see, e.g., [5], [16]) and the elements of  $\mathbf{H}_c$  are correlated in these cases. Ignoring channel statistics would cause mismatch in capacity assessment and code design. Exploitation of channel statistics, on the other hand, could significantly enhance code design and performance.

The virtual channel representation is a novel channel modeling approach that connects idealistic statistic models and parametric physical models [5]. It imposes structure on the channel matrix  $\mathbf{H}_c$  by capturing essential characteristics of the physical scattering environment. To illustrate the virtual channel representation, we focus on one-dimensional uniform linear arrays (ULA's) of antennas at both the transmitter and receiver and consider far-field scattering characteristics. Let  $d_T$  and  $d_R$  denote the antenna spacing at the transmitter and receiver, respectively. The channel matrix can be described via array steering and response vectors given by

$$\begin{aligned} \mathbf{a}_T(\theta_T) &= \frac{1}{\sqrt{M}} \left( 1, e^{-j2\pi\theta_T}, \dots, e^{-j2\pi(M-1)\theta_T} \right)^\top \\ \mathbf{a}_R(\theta_R) &= \frac{1}{\sqrt{N}} \left( 1, e^{-j2\pi\theta_R}, \dots, e^{-j2\pi(N-1)\theta_R} \right)^\top \end{aligned} \quad (2)$$

where  $\theta$  is related to the beam angle  $\varphi$ , the angle between the beam direction and the horizontal axis (see Fig. 1), as  $\theta = d \sin(\varphi) / \lambda$  with  $\lambda$  being the wavelength of propagation. The vector  $\mathbf{a}_R(\theta_R)$  represents the signal response at the receiver array due to a point source in the direction  $\theta_R$ . Similarly  $\mathbf{a}_T(\theta_T)$  represents the array weights needed to transmit a beam focused in the direction of  $\theta_T$ .

The finite dimensionality of the spatial signal space<sup>1</sup> can be exploited to develop a *linear* virtual channel representation that uses spatial beams in fixed, virtual directions [5]. The virtual channel representation, illustrated in Fig. 1, can be expressed as

$$\mathbf{H}_c = \sum_{m=1}^M \sum_{n=1}^N H_V(m, n) \mathbf{a}_R(\theta_{R,m}) \mathbf{a}_T^\dagger(\theta_{T,n}) = \mathbf{A}_R \mathbf{H}_V \mathbf{A}_T^\dagger \quad (3)$$

<sup>1</sup>Due to finite number of antenna elements and finite array aperture.

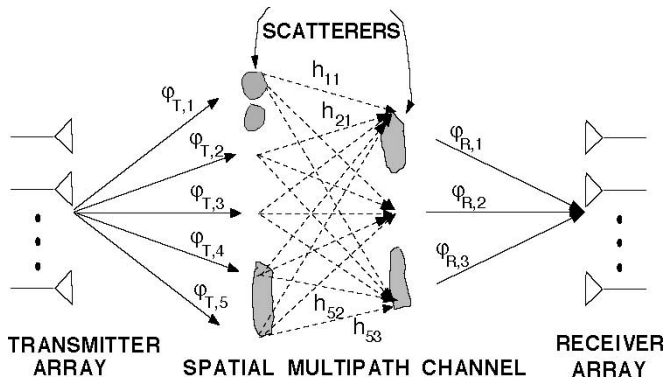


Fig. 1. Schematic illustrating virtual representation of the scattering environment. The virtual angles are fixed *a priori* and their spacing is determined by the antenna spacing and defines the spatial resolution. The virtual channel matrix  $\mathbf{H}_V$  consists of coupling between virtual transmit/receive beams in the direction of virtual angles.

where  $\{\theta_{R,m}\}$  and  $\{\theta_{T,n}\}$  are fixed virtual angles that result in full-rank matrices

$$\begin{aligned} \mathbf{A}_R &= (\mathbf{a}_R(\theta_{R,1}), \dots, \mathbf{a}_R(\theta_{R,M})) (M \times M) \\ \mathbf{A}_T &= (\mathbf{a}_T(\theta_{T,1}), \dots, \mathbf{a}_T(\theta_{T,N})) (N \times N). \end{aligned} \quad (4)$$

The  $M \times N$  matrix  $\mathbf{H}_V$  is the virtual channel matrix. Uniform sampling of the principal period  $\theta \in [-0.5, 0.5]$  is a natural choice for virtual spatial angles, which yields unitary matrices  $\mathbf{A}_R$  and  $\mathbf{A}_T$ —discrete Fourier transform (DFT) matrices—in (4). Since  $\mathbf{A}_R$  and  $\mathbf{A}_T$  are unitary,  $\mathbf{H}_V$  is related to  $\mathbf{H}$  as

$$\mathbf{H}_V = \mathbf{A}_R^\dagger \mathbf{H}_c \mathbf{A}_T \quad (5)$$

and, thus,  $\mathbf{H}_V$  is unitarily equivalent to  $\mathbf{H}_c$  and captures all channel information. In fact,  $\mathbf{H}_V$  is a two-dimensional DFT of  $\mathbf{H}_c$ .

Realistic scattering environments can be modeled via a superposition of scattering clusters with limited angular spreads (see, e.g., [5], [16]). The virtual channel matrix  $\mathbf{H}_V$  provides an intuitively appealing representation for such environments (see Fig. 2): different clusters correspond to different nonvanishing submatrices of  $\mathbf{H}_V$ . Furthermore, it is shown in [5] that the nonvanishing elements of  $\mathbf{H}_V$  are approximately uncorrelated under the usual assumption of uncorrelated physical scattering. Virtual channel representation clearly reveals the key channel characteristics affecting capacity: the number of parallel channels can be determined by the size/rank of virtual submatrices corresponding to different clusters, and the level of diversity is determined by the nature of scattering in each cluster.

We next propose a  $K$ -diagonal channel model, a refined version of the one proposed in [5], which forms the centerpiece of the study in this paper and also illustrates the power of the virtual representation framework. We assume virtual matrix  $\mathbf{H}_V$  to be full rank since the problem can be reduced to a lower dimensional case otherwise. Consider a single cluster covering the entire spatial horizon. On one extreme is “diagonal scattering” ( $\mathbf{H}_V$  approximately diagonal), illustrated in Fig. 3(a), in which each transmit virtual angle couples with only one corresponding virtual receive angle. As argued in [5], this corresponds to high correlation and lower diversity per parallel channel. On the other extreme is “maximally rich scattering” (all elements of  $\mathbf{H}_V$  non-

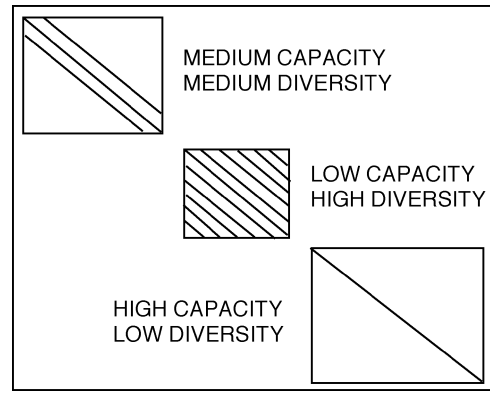


Fig. 2. Schematic depicting decomposition of  $\mathbf{H}_V$  for a clustered scattering environment into nonvanishing submatrices (with uncorrelated entries) corresponding to the different clusters. Each submatrix is in turn modeled as a  $K$ -diagonal matrix reflecting the nature of scattering in the cluster. The size of each matrix determines the capacity supported by the cluster whereas the number of diagonals represents the diversity afforded by the cluster.

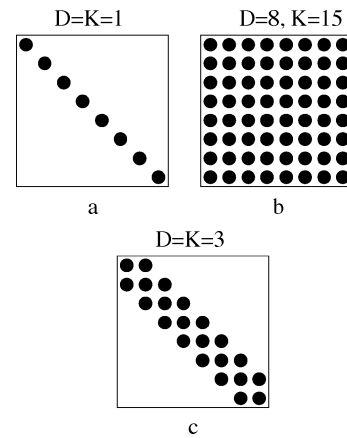


Fig. 3. Illustration of  $K$ -diagonal channels via  $\mathbf{H}_V$  where  $K$  is the number of nonvanishing diagonals and  $D$  is the diversity per dimension. (a) “Diagonal” scattering depicting a line of point scatters between the transmitter and receiver—each virtual transmit angle couples with only a few corresponding virtual receive angles. (b) “Maximally” rich scattering environment in which each virtual transmit angle couples with nearly all virtual receive angles. (c)  $K$ -diagonal channel encompassing the two extremes.

vanishing), illustrated in Fig. 3(b), in which each virtual transmit angle couples with all virtual receive angles. This corresponds to minimum correlation (i.i.d. channels) and maximum diversity. Spanning the above two extremes is the  $K$ -diagonal channel as illustrated in Fig. 3(c). Varying  $K$ , the number of nonvanishing diagonals in  $\mathbf{H}_V$ , captures various levels of diversity per dimension ranging from the lowest to the highest. Equivalently, it captures various level of channel correlation from highest ( $K = 1$ ) to lowest (maximum  $K$ ). The diversity per parallel channel indexed by  $K$  significantly affects channel capacity, particularly outage capacity [17]. However, study in [5] confirmed the well-known diminishing return due to diversity, that is, a few diagonals are sufficient to capture a major portion of available channel diversity. Therefore,  $K$ -diagonal channel represents a practical approximation to the actual channel as well. Based on the concept of  $K$ -diagonal channels, general virtual channels could be approximated by a concatenation of various  $K$ -diagonal subchannels, as shown in Fig. 2, where each sub-channel may have different dimensions, diversity, and power.

For better exposition of  $K$ -diagonal channels, we have the following definition.

*Definition 1:* Suppose the virtual channel matrix  $\mathbf{H}_V$  has dimension  $M \times N$ . The  $K$ -diagonal (virtual) channel is defined as

$$H_V(m, n) \sim \begin{cases} \text{CN}^1(0, \sigma^2), & \text{if } k_1 \leq m - n \leq k_2 \\ 0, & \text{otherwise} \end{cases} \quad (6)$$

where  $K = k_2 - k_1 + 1$  is the total number of nonvanishing diagonals in  $\mathbf{H}_V$  and  $\sigma^2$  is the variance of nonvanishing elements. The *diversity degree* of the  $K$ -diagonal channel is

$$D_N(K) = \max_{1 \leq m \leq M} \text{card}(\mathcal{A}_m) = \begin{cases} K, & \text{if } K \leq N \\ N, & \text{otherwise} \end{cases} \quad (7)$$

where  $\mathcal{A}_m$  is the set of nonvanishing elements in the  $m$ th row of  $\mathbf{H}_V$  and  $\text{card}(\mathcal{A}_m)$ , the cardinality of  $\mathcal{A}_m$ , is the number of elements in the set  $\mathcal{A}_m$ .

The  $K$ -diagonal channel together with its diversity degree is depicted in Fig. 3. In the following, we abbreviate  $D_N(K)$  as  $D$  if there is no confusion. The diversity degree of a  $K$ -diagonal channel indicates the diversity level per dimension, that is, the maximum diversity seen by a receive virtual angle. As evident from (7),  $D = K$  in most cases except when  $K$  is larger than  $N$ . As  $K$  varies from 1 to  $M + N - 1$  ( $D$  varies from 1 to  $N$  correspondingly), the channel changes from  $M$ -parallel Rayleigh fading channels with no diversity to the  $M \times N$  idealistic i.i.d. channel with maximum diversity.

### III. SPACE-TIME $D$ -BLOCK CODES

As elaborated in Section II, virtual channel representation offers a unique modeling advantage over existing methods in that insights from physical scattering characteristics and the convenience of uncorrelated statistical modeling can be combined. The nonvanishing approximately uncorrelated elements of  $\mathbf{H}_V$  are the essential degrees of freedom in the channel. The approximately uncorrelated nature of virtual matrix elements greatly facilitates code design and performance analysis. Our aim is to exploit the channel (statistical) structure revealed by  $\mathbf{H}_V$  for improved space-time codes design. Hence, our codes assume only channel statistics at the transmitter while channel realization is assumed at the receiver for coherent detection. We focus on the  $K$ -diagonal model because it is the basic building block for approximating general correlated channel structures as discussed in the previous section.

The virtual channel representation naturally suggests code design and analysis in the virtual (Fourier) domain by virtue of the unitary DFT matrices  $\mathbf{A}_R$  and  $\mathbf{A}_T$  in (3). The received signal is transformed as

$$\mathbf{y} = \mathbf{A}_R^\dagger \mathbf{r} = \mathbf{H}_V \mathbf{A}_T^\dagger \mathbf{s} + \mathbf{A}_R^\dagger \mathbf{z} = \sqrt{E_s} \mathbf{H}_V \mathbf{x} + \mathbf{z} \quad (8)$$

where  $\mathbf{s} = \sqrt{E_s} \mathbf{A}_T \mathbf{x}$  can be regarded as DFT precoding of the input  $\mathbf{x}$ . The power constant  $E_s$  in (8) normalizes the transmit constellation to have unit power. Without loss of generality, we assume that elements in  $\mathbf{H}_V$  have unit power and that the noise  $\mathbf{z} \sim \text{CN}^M(\mathbf{0}, \mathbf{I})$  is temporally independent. The signal-to-noise ratio (SNR) of the system is defined by  $\text{SNR} = NE_s$  so that SNR is fixed regardless of the number of transmit antennas. In the following, we always refer to (8) as the (virtual) channel

equation without explicitly mentioning the unitary transformations at the transmitter and receiver. Note that the setup in (8) differs from conventional approaches only in that  $\mathbf{H}_V$  exhibits certain structure dictated by the physical scattering characteristics. We also refer to the input dimensions and output dimensions of the MIMO equation generally as transmit elements and receive elements, which may correspond to antenna elements in the conventional channel representation (1) or to virtual beams in the virtual channel representation (5), depending on the context.

#### A. Design Criteria for Virtual Channel Coding

Before discussing coding for the  $K$ -diagonal channel, we give a design criterion for general correlated MIMO channels based on pairwise error probability (PEP) analysis following the approach in [3]. We assume that the transmitter and receiver have knowledge of the parameter  $K$  which characterizes correlation/diversity in the  $K$ -diagonal model as well as matrices  $\mathbf{A}_T$  and  $\mathbf{A}_R$  in the model. A space-time code  $\mathcal{X}$  consists of various  $L \times N$  matrices where  $N$  and  $L$  are the span of codewords in space and time, respectively. More specifically, the  $(l, n)$ -th element in a codeword  $\mathbf{X}$  is the signal transmitted at the  $n$ -th transmit element and at the  $l$ -th discrete time. The received signal due to a codeword can be written as

$$\mathbf{Y} = \sqrt{E_s} \mathbf{X} \mathbf{H} + \mathbf{Z} \quad (9)$$

where  $\mathbf{H} = \mathbf{H}_V^\top$  in the virtual channel case and  $\mathbf{Y}/\mathbf{Z}$  is a stack of received signal/noise at the receiver.

The PEP,  $P(\mathbf{X} \rightarrow \hat{\mathbf{X}})$ , of decoding codeword  $\hat{\mathbf{X}}$  instead of  $\mathbf{X}$ , is given by

$$P(\mathbf{X} \rightarrow \hat{\mathbf{X}}) = \mathbf{E} \left[ Q \left( \sqrt{\frac{E_s}{2}} \left\| (\mathbf{X} - \hat{\mathbf{X}}) \mathbf{H} \right\|_F \right) \right] \quad (10)$$

where  $Q(x) = \int_x^\infty e^{-(t^2/2)} dt$  is the Gaussian tail integration function and the expectation is with respect to the random  $\mathbf{H}$ .

*Theorem 1:* Let  $\mathbf{R}_\Delta = (\mathbf{X} - \hat{\mathbf{X}})^\dagger (\mathbf{X} - \hat{\mathbf{X}})$ , and let  $\mathbf{R} = \mathbf{E}[\text{vec}(\mathbf{H}) \text{vec}(\mathbf{H})^\dagger]$ . The PEP is upper bounded by

$$P(\mathbf{X} \rightarrow \hat{\mathbf{X}}) \leq \frac{1}{\det(\mathbf{I}_{MN} + \frac{E_s}{4} \mathbf{R} (\mathbf{I}_M \otimes \mathbf{R}_\Delta))}. \quad (11)$$

*Proof:* Applying the inequality  $Q(x) \leq e^{-(x^2/2)}$  to (10), one has

$$\begin{aligned} P(\mathbf{X} \rightarrow \hat{\mathbf{X}}) &\leq \mathbf{E} \left[ \exp \left( -\frac{E_s}{4} \left\| (\mathbf{X} - \hat{\mathbf{X}}) \mathbf{H} \right\|_F^2 \right) \right] \\ &= \mathbf{E} \left[ \exp \left( -\frac{E_s}{4} \mathbf{h}^\dagger (\mathbf{I}_M \otimes \mathbf{R}_\Delta) \mathbf{h} \right) \right] \end{aligned} \quad (12)$$

where  $\mathbf{h} = \text{vec}(\mathbf{H}) \sim \text{CN}^{MN}(\mathbf{0}, \mathbf{R})$ . The upper bound in (11) results from evaluating the quadratic term in (12). However, caution must be taken when  $\mathbf{h}$  is degenerate, that is,  $\mathbf{R}$  is not of full rank, especially for the virtual channel representation where vanishing elements in  $\mathbf{H}_V$  contribute to rank deficiency.

First, suppose  $\mathbf{R}$  is of full rank. The Gaussian probability density function of  $\mathbf{h}$  is

$$f(\mathbf{h}) = \frac{1}{\pi^{MN} \det \mathbf{R}} \exp(-\mathbf{h}^\dagger \mathbf{R}^{-1} \mathbf{h}). \quad (13)$$

Therefore, the expectation in (12) can be computed as

$$\frac{1}{\pi^{MN} \det \mathbf{R}} \int \exp \left( -\mathbf{h}^\dagger \left( \frac{E_s}{4} (\mathbf{I}_M \otimes \mathbf{R}_\Delta) + \mathbf{R}^{-1} \right) \mathbf{h} \right) d\mathbf{h}. \quad (14)$$

Since  $\mathbf{R}^{-1}$  is positive definite and  $\mathbf{I}_M \otimes \mathbf{R}_\Delta$  is nonnegative definite, the sum  $(E_s/4)(\mathbf{I}_M \otimes \mathbf{R}_\Delta) + \mathbf{R}^{-1}$  is positive definite. In particular, it is invertible. Let  $\tilde{\mathbf{R}}^{-1} = (E_s/4)(\mathbf{I}_M \otimes \mathbf{R}_\Delta) + \mathbf{R}^{-1}$ . One has

$$\begin{aligned} \text{RHS of (14)} &= \frac{1}{\pi^{MN} \det \mathbf{R}} \int \exp(-\mathbf{h}^\dagger \tilde{\mathbf{R}}^{-1} \mathbf{h}) d\mathbf{h} \\ &= \frac{\det \tilde{\mathbf{R}}}{\det \mathbf{R}} \\ &= \frac{1}{\det (\mathbf{I}_{MN} + \frac{E_s}{4} \mathbf{R} (\mathbf{I}_M \otimes \mathbf{R}_\Delta))} \end{aligned} \quad (15)$$

by using Gaussian integration

$$\int \exp(-\mathbf{h}^\dagger \tilde{\mathbf{R}}^{-1} \mathbf{h}) d\mathbf{h} = \pi^{MN} \det \tilde{\mathbf{R}}.$$

Thus, we have proved the theorem for the case when  $\mathbf{R}$  is invertible.

Next, suppose  $\mathbf{R}$  is singular and let  $r = \text{rank} \mathbf{R}$ . The eigenvalue decomposition [15] gives  $\mathbf{h} = \mathbf{U}\mathbf{v}$  with  $\mathbf{R} = \mathbf{U}\mathbf{\Lambda}\mathbf{U}^\dagger$  where the  $r$ -dimensional  $\mathbf{v} \sim \text{CN}^r(0, \mathbf{\Lambda})$ . One has

$$\begin{aligned} \text{RHS of (12)} &= \mathbf{E} \left[ \exp \left( -\frac{E_s}{4} \mathbf{v}^\dagger \mathbf{U}^\dagger (\mathbf{I}_M \otimes \mathbf{R}_\Delta) \mathbf{U} \mathbf{v} \right) \right] \\ &\stackrel{(a)}{=} \frac{1}{\det (\mathbf{I}_r + \frac{E_s}{4} \mathbf{\Lambda} \mathbf{U}^\dagger (\mathbf{I}_M \otimes \mathbf{R}_\Delta) \mathbf{U})} \\ &\stackrel{(b)}{=} \frac{1}{\det (\mathbf{I}_{MN} + \frac{E_s}{4} \mathbf{U} \mathbf{\Lambda} \mathbf{U}^\dagger (\mathbf{I}_M \otimes \mathbf{R}_\Delta))} \\ &= \frac{1}{\det (\mathbf{I}_{MN} + \frac{E_s}{4} \mathbf{R} (\mathbf{I}_M \otimes \mathbf{R}_\Delta))} \end{aligned}$$

where (a) is obtained by applying the previous calculations on the nondegenerate Gaussian vector  $\mathbf{v}$  and (b) follows from  $\det(\mathbf{I} + \mathbf{A}\mathbf{B}) = \det(\mathbf{I} + \mathbf{B}\mathbf{A})$  [15]. ■

*Remark 1:* The upper bound derived above is the standard Chernoff bound applied to the correlated channel. Tighter bounding techniques such as the one in [18] and [10] have been reported in the literature. However, our bound exposes the interaction of channel structure ( $\mathbf{R}$ ) and code property ( $\mathbf{R}_\Delta$ ) in a simple form that facilitates the subsequent code design for correlated channels.

Theorem 1 generalizes the methods of [3] to correlated channels. In the case of the idealistic i.i.d. channel,  $\mathbf{R} = \mathbf{I}_{MN}$  in (11), which gives rise to the well-known rank and determinant criteria in [3]

$$P(\mathbf{X} \rightarrow \hat{\mathbf{X}}) \leq \frac{1}{\left( \prod_{i=1}^{r_\Delta} \left( 1 + \frac{\lambda_i E_s}{4} \right) \right)^M} \quad (16)$$

where  $\lambda_1, \dots, \lambda_{r_\Delta}$  are the nonzero eigenvalues of  $\mathbf{R}_\Delta$ . Thus, a diversity advantage of  $Mr_\Delta$  and a coding advantage of  $(\lambda_1 \cdots \lambda_{r_\Delta})^{1/r_\Delta}$  are achieved. The design criteria for the i.i.d. channel depend solely on the properties of space-time codes or codeword differences. However, in generally correlated channels, channel correlation matrix  $\mathbf{R}$  is no longer an identity matrix and comes into play in the term  $\mathbf{R}(\mathbf{I}_M \otimes \mathbf{R}_\Delta)$  in (11).

The interaction between channel statistics and space-time code properties necessitates a combined approach that accounts for channel structure as well as space-time code properties. However, such an interaction may be very complicated especially when  $\mathbf{R}$  itself exhibits no ‘‘simple’’ form. As we have seen in Section II, the virtual channel representation actually ‘‘decorrelates’’ the channel, yielding a diagonal matrix  $\mathbf{R}$ , which simplifies code design in many cases. Next, we present a class of space-time codes for  $K$ -diagonal channels, space-time  $D$ -block codes, that are tuned to the  $K$ -diagonal channel structure and can serve as building blocks for more general virtual channel coding. Our results demonstrate that significant benefits can be reaped by taking advantage of the channel structure revealed by the virtual representation.

### B. Construction of Space-Time $D$ -Block Codes

Space-time  $D$ -block codes are, as the name suggested, essentially the space-time block codes invented by Tarokh *et al.* [11] adapted to  $K$ -diagonal virtual channels. Codewords of space-time block codes are  $L \times N$  matrices consisting of linear combinations of  $Q$  transmitted symbols and their conjugates. The corresponding transmission rate is  $Q/L$  complex symbols per channel use. Such a code entails a delay of  $L$  discrete time units. The design for space-time block codes is anchored on the theory of orthogonal designs [19], which is used to construct orthogonal codewords regardless of particular values of transmitted symbols. More specifically, let  $c_1, \dots, c_Q$  be the transmitted symbols. Every codeword satisfies  $\mathbf{X}^\dagger \mathbf{X} = (\sum_{q=1}^Q |c_q|^2) \mathbf{I}_N$ . Therefore, it follows that

$$\mathbf{R}_\Delta = (\mathbf{X} - \hat{\mathbf{X}})^\dagger (\mathbf{X} - \hat{\mathbf{X}}) = \left( \sum_{q=1}^Q |c_q - \hat{c}_q|^2 \right) \mathbf{I}_N \quad (17)$$

by the linearity of the code. Substituting (17) into (11), one can compute the PEP as

$$P(\mathbf{X} \rightarrow \hat{\mathbf{X}}) \leq \frac{1}{\det \left( \mathbf{I}_{MN} + \frac{E_s}{4} \left( \sum_{q=1}^Q |c_q|^2 \right) \mathbf{R} \right)} \quad (18)$$

which shows that space-time block codes are capable of attaining full diversity afforded by the channel. For the convenience of exposition, we denote by  $\mathcal{G}^N$  a space-time block code for  $N$  transmit elements. Generally speaking, the minimal delay  $L$  for which  $\mathcal{G}^N$  exists is  $d(2N)$  where  $d(\cdot)$  is defined in the following [11], [20].

*Definition 2:* Let  $l = 2^a b$ , where  $b$  is odd and  $a = 4c + d$  with  $0 \leq d < 4$  and  $0 \leq c$ . The function  $\rho(l)$  is defined as  $\rho(l) = 8c + 2^d$ . We define

$$d(n) = \min \{ l : \rho(l) \geq n \}. \quad (19)$$

Note that  $d(n)$  grows very fast as  $n$  increases [19]. A large delay will be incurred by space-time block codes as the cost of achieving full diversity. One can also see from (18) that space-time block codes are insensitive to channel structure. In particular, the delay is fixed by orthogonal designs and is independent of channel structure. For a structured channel such as the  $K$ -diagonal channel, the stringent orthogonality requirement in space-time block codes may be relaxed. Next, we propose one such scheme that achieves full diversity but

with significantly less delay than space-time block codes for  $K$ -diagonal channels.

*Theorem 2 (Full Diversity Achieving Property):* For a full diversity achieving code for  $K$ -diagonal channels, it is sufficient that every  $D = D_N(K)$  consecutive columns of its codeword difference matrices  $\mathbf{X} - \hat{\mathbf{X}}$  are linearly independent, while the whole matrix can be rank-deficient. In contrast, space-time block codes require all codeword difference matrices to be of full rank.

*Proof:* Denote by  $\mathbf{h}_m$  the  $m$ th column of  $\mathbf{H}$  in (9). Theorem 1 can be simplified due to decorrelation of virtual channel coefficients as

$$\text{RHS of (11)} = \frac{1}{\prod_{m=1}^M \det(\mathbf{I}_N + \frac{E_s}{4} \mathbf{R}_m \mathbf{R}_\Delta)} \quad (20)$$

where  $\mathbf{R}_m = \mathbf{E}[\mathbf{h}_m \mathbf{h}_m^\dagger]$  is a diagonal matrix in the virtual representation. Since every column of  $\mathbf{H}$  contains  $D = D_N(K)$  nonvanishing elements in  $K$ -diagonal channels, one has  $\mathbf{R}_m = \text{diag}(\mathbf{0}_s, \mathbf{I}_D, \mathbf{0}_t)$  with  $s + D + t = N$ ,  $s, t \geq 0$ . Partition  $\mathbf{R}_\Delta$  correspondingly according to  $\mathbf{R}_m$  and denote  $\mathbf{R}_{\Delta,D} = (\mathbf{X} - \hat{\mathbf{X}})_D^\dagger (\mathbf{X} - \hat{\mathbf{X}})_D$ , that is, the outer product of corresponding  $D$  consecutive columns of  $\mathbf{X} - \hat{\mathbf{X}}$ . Therefore,

$$\det\left(\mathbf{I}_N + \frac{E_s \mathbf{R}_m \mathbf{R}_\Delta}{4}\right) = \det\left(\mathbf{I}_D + \frac{E_s \mathbf{R}_{\Delta,D}}{4}\right) \quad (21)$$

which, combined with (20), establishes the theorem.  $\blacksquare$

For a  $K$ -diagonal channel with  $N$  transmit elements, we first choose a space-time block code  $\mathcal{G}^D$  for  $D = D_N(K)$  (virtual) transmit elements. The space-time  $D$ -block code  $\mathcal{C}^{(D,N)}$  generated by  $\mathcal{G}^D$  is illustrated in Fig. 4. Incoming information symbols first form a  $L \times D$  codeword  $\mathcal{G}^D$ . The corresponding  $L \times N$  codeword  $\mathcal{C}^{(D,N)}$  is obtained by repeating  $\mathcal{G}^D$  until  $N$  columns have been filled. More specifically, denote by  $\mathcal{G}_d^D$  and  $\mathcal{C}_n^{(D,N)}$  the  $d$ -th column of  $\mathcal{G}^D$  and the  $n$ th column of  $\mathcal{C}^{(D,N)}$ , respectively. Then

$$\mathcal{C}_n^{(D,N)} = \mathcal{G}_{(n)_D}^D \quad (22)$$

where  $(n)_D$  is the remainder of  $n$  divided by  $D$ . The modular operation in (22) implies that any  $D$  consecutive columns of the space-time  $D$ -block code form its generating space-time block code (see Fig. 4). For example, suppose  $\mathcal{G}^3$  has three columns, denoted as (1,2,3). Then  $\mathcal{C}^{(3,6)}$  can be represented as (1,2,3,1,2,3). One can easily check that any three consecutive columns of  $\mathcal{C}^{(3,6)}$  are (1,2,3) or its cyclic shift. Since receive elements are coupled with at most  $D$  consecutive transmit elements in  $K$ -diagonal channels, they essentially see the same space-time block code  $\mathcal{G}^D$ . It follows that the code rate and delay of a space-time  $D$ -block code  $\mathcal{C}^{D,N}$  are those of its generating space-time block code  $\mathcal{G}^D$ .

From this construction, space-time  $D$ -block codes are generally nonorthogonal. However, any  $D$  consecutive columns of a space-time  $D$ -block codeword are orthogonal since they actually form a space-time block codeword. Thus, the characterization in Theorem 2 shows that space-time  $D$ -block codes achieve full diversity over  $K$ -diagonal channels. We give a few examples of space-time  $D$ -block codes whose generating space-time block codes are chosen from [11].

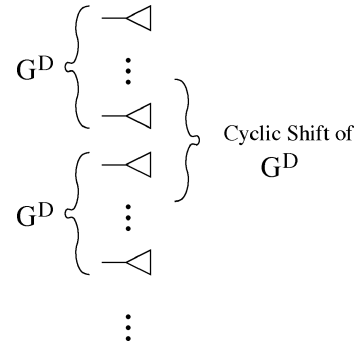


Fig. 4. Schematic illustration of encoding for space-time  $D$ -block codes. The generating space-time block code is duplicated every  $D = D_N(K)$  transmit elements. Signals from any  $D$  consecutive transmit elements form the generating space-time block code or its cyclic shift.

*Example 1 (Space-Time 2-Block Code for  $4 \times 4$  Channels):*

$$\mathcal{G}^2 = \begin{pmatrix} c_1 & c_2 \\ -c_2^* & c_1^* \end{pmatrix}, \quad \mathcal{C}^{(2,4)} = \begin{pmatrix} c_1 & c_2 & c_1 & c_2 \\ -c_2^* & c_1^* & -c_2^* & c_1^* \end{pmatrix} \quad (23)$$

where  $\mathcal{G}^2$  is the Alamouti scheme [21]. The code has rate 1 and delay 2.

*Example 2 (Space-Time 3-Block Code for  $4 \times 4$  Channels):*

$$\mathcal{G}^3 = \begin{pmatrix} c_1 & c_2 & \frac{c_3}{\sqrt{2}} \\ -c_2^* & c_1^* & \frac{c_3}{\sqrt{2}} \\ \frac{c_3}{\sqrt{2}} & \frac{c_3}{\sqrt{2}} & \frac{(-c_1 - c_1^* + c_2 - c_2^*)}{2} \end{pmatrix}$$

$$\mathcal{C}^{(3,4)} = \begin{pmatrix} c_1 & c_2 & \frac{c_3}{\sqrt{2}} & c_1 \\ -c_2^* & c_1^* & \frac{c_3}{\sqrt{2}} & -c_2^* \\ \frac{c_3}{\sqrt{2}} & \frac{c_3}{\sqrt{2}} & \frac{(-c_1 - c_1^* + c_2 - c_2^*)}{2} & \frac{c_3}{\sqrt{2}} \\ \frac{c_3}{\sqrt{2}} & -\frac{c_3}{\sqrt{2}} & \frac{(c_2 + c_2^* + c_1 - c_1^*)}{2} & \frac{c_3}{\sqrt{2}} \end{pmatrix} \quad (24)$$

which has rate 3/4 and delay 4.

Space-time  $D$ -block codes demonstrate the advantage of virtual channel representation. The intrinsic channel structure is obscured under conventional channel representation where channel matrix has generally correlated elements. So, a space-time block code  $\mathcal{G}^N$  needs to be used in order to achieve full diversity on an antenna array with  $N$  transmit elements. However, if the virtual channel representation is used instead, the  $K$ -diagonal structure will be clearly revealed based on which a space-time block code  $\mathcal{G}^D$  is sufficient to achieve the same performance. Since  $d(2D_N(K)) \leq d(2N)$ , coding in virtual channel domain offers smaller delay. And such delay saving can be very substantial if the channel matrix is sparse, that is,  $K \ll N$ . Furthermore, a space-time  $D$ -block code can adapt to channel structure. As  $K$  increases, it eventually coincides with a space-time block code for  $N$  antennas. We would like to emphasize that space-time  $D$ -block codes are one particular (simple) scheme based on space-time block codes to fit  $K$ -diagonal channels.

### C. Decoding of Space-Time $D$ -Block Codes

We first present a decoding method that captures the essence of space-time block codes. Consider a space-time block code  $\mathcal{G}^N$  with delay  $L$  and symbol rate  $R$ . Hence, a total of  $Q = RL$

complex symbols  $c_1, \dots, c_Q$  are encoded in one codeword. The signal at a particular receive element and at discrete time  $t$  can be expressed as

$$r_t = \sum_{n=1}^N h_n s_n + w_t \quad (25)$$

where  $s_n$ 's are transmitted symbols coded by  $\mathcal{G}^N$ . Write  $\mathbf{r} = (r_1^R, r_1^I, \dots, r_L^R, r_L^I)^\top$  (and similarly for  $\mathbf{c}$  and  $\mathbf{w}$ ) where  $(\cdot)^R$  and  $(\cdot)^I$  denote the real and imaginary part of a complex variable, respectively. Space-time block codes can be represented as linear dispersion codes [13] as

$$\mathbf{r} = \mathcal{H}\mathbf{c} + \mathbf{w} \quad (26)$$

where  $\mathcal{H}$  is a  $2L \times 2Q$  matrix whose elements are linear combinations of channel coefficients  $h_1^R, h_1^I, \dots, h_N^R, h_N^I$ . Space-time block codes cleverly design  $\mathcal{H}$  to be orthogonal, that is,  $\mathcal{H}^\dagger \mathcal{H} = (\sum_{n=1}^N |h_n|^2) \mathbf{I}_{2Q}$  through orthogonal designs [13], [20], [22]. The orthogonality of  $\mathcal{H}$  in (26) greatly simplifies the decoding of space-time block codes—multiplying the received signal by  $\mathbf{U} = (1)/(\sqrt{|h_1|^2 + \dots + |h_N|^2}) \mathcal{H}^\dagger$ , one has

$$\mathbf{y} = \mathbf{U} \mathcal{H}^\dagger \mathbf{r} = \left( \sum_{n=1}^N |h_n|^2 \right)^{\frac{1}{2}} \mathbf{c} + \mathbf{z} \quad (27)$$

where  $\mathbf{z} = \mathbf{U} \mathcal{H}^\dagger \mathbf{w} \sim \text{CN}^{2Q}(0, \mathbf{I}_{2Q})$ . Since  $\sum_{n=1}^N |h_n|^2 \sim \chi_{2N}^2$ , space-time block codes convert the original vector channel into a scalar channel with  $N$  level of diversity. The conversion is transparent in that additional coding techniques for the diversity scalar channel can be applied to the transmitted symbols to further enhance performance. The corresponding decoding can be easily done after space-time coded symbols are demodulated as above.

Since space-time  $D$ -block codes are essentially space-time block codes, it is not surprising that they preserve the simple decoding algorithm as that of space-time block codes. The trick here is to notice that although codewords of space-time  $D$ -block codes are not orthogonal, every receive element can only “see” a portion of codeword, actually its  $D = D_N^K$  consecutive columns. However, these columns form a codeword of the underlining space-time block code. So, they can be decoded by the above algorithm. We illustrate the decoding algorithm for space-time  $D$ -block codes in Fig. 5. Suppose  $\mathcal{C}^{(D,N)}$  is generated by  $\mathcal{G}^D$ . For each receive element, the corresponding  $\mathcal{G}^D$  or its cyclic shift is demodulated. Then, all the decoding branches for the same symbol are combined using maximum ratio combining [23] to form final demodulated symbol. Therefore, it can be easily verified from (27) that space-time  $D$ -block codes and space-time block codes both convert the original  $K$ -diagonal channel into the same scalar channel

$$\mathbf{y} = \|\mathbf{H}\|_{\mathcal{F}} \mathbf{c} + \mathbf{z}. \quad (28)$$

We simulated the performance of space-time  $D$ -block codes over a  $4 \times 4$  MIMO channel with  $K = 2$  and  $K = 3$ . The corresponding  $K$ -diagonal channels are simulated directly in the virtual domain to illustrate coding performance. The

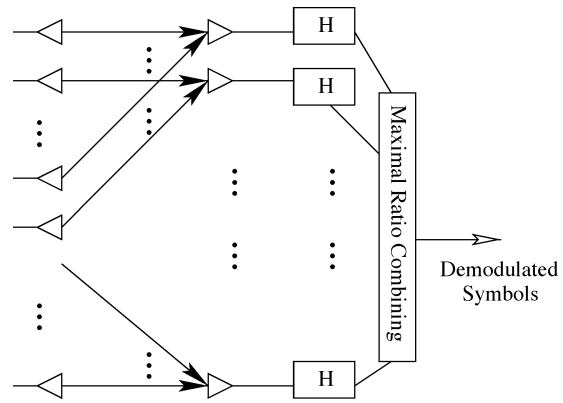


Fig. 5. Schematic illustration of decoding for space-time  $D$ -block codes. The demodulation for the corresponding space-time block code is performed at every receive element. All the receive branches are then combined using maximal ratio combining to generate the final decoded symbol.

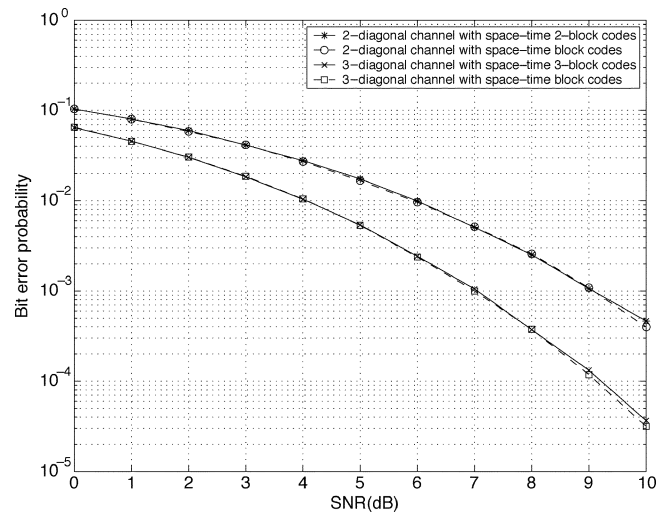


Fig. 6. Bit-error probability of space-time  $D$ -block codes and space-time block codes on  $4 \times 4$   $K$ -diagonal channels with  $K = 2$  and  $K = 3$ . 4QAM is used at every transmit element. A frame consists of 400 symbols. Both codes offer identical performance but space-time  $D$ -block codes require less delay than space-time block codes while delivering a higher rate at the same time.

space-time  $D$ -block codes are taken from Example 1 and Example 2. Data are transmitted in frames of 400 symbols. The four quadrature amplitude modulation (4QAM) is used at each transmit antenna. Channel remains constant over one frame but changes independently from one frame to another. As a comparison, space-time block codes are applied under the conventional channel representation. Fig. 6 plots the bit-error rate (BER) of different codes. It is evident that space-time  $D$ -block codes and space-time block codes yield almost identical performance. However, space-time two-block codes provide a rate of one complex symbol per channel use with a delay of two time units, while space-time block codes with four transmit dimensions can only provide 3/4 complex symbol per channel use with a delay of four [11]. Note that in this specific example space-time  $D$ -block codes yield higher data rate than space-time block codes with the same transmit dimension while yielding nearly identical BER. Similar to space-time block codes, space-time  $D$ -block codes achieve full diversity but the knowledge of channel structure allows one to properly

design a space-time  $D$ -block code that incurs much smaller delay in general.

#### IV. VIRTUAL ANGLE GROUPING

One prominent structure of a space-time  $D$  block code is its periodicity which admits a simple interpretation via virtual angle grouping. According to the construction of space-time  $D$ -block code (22), the generating code  $\mathcal{G}^D$ , which spans  $D$  spatial virtual angles, repeats itself in spatial dimension. Such spatial periodicity implies that transmitted signals are identical at two virtual angles provided the virtual angles are separated by  $D$  apart. Mathematically, let  $x_n$  for  $1 \leq n \leq N$  be the transmitted signal at the  $n$ th virtual angle, one has

$$x_i = x_j, \quad \text{if } i \equiv j \pmod{D}. \quad (29)$$

Denote by  $\{d\}_D^N$  the  $d$ th modular class of  $D$  in  $N$ , that is

$$\{d\}_D^N = \{1 \leq n \leq N | n \equiv d \pmod{D}\}. \quad (30)$$

It follows from (29) that virtual angles in the same modular class are grouped together. In other words, the same signal is transmitted at every virtual angle in the same modular class. From (8), the  $m$ th received signal can now be written as

$$\begin{aligned} y_m &= \sqrt{E_S} \sum_{n=1}^N [\mathbf{H}_V]_{m,n} x_n + z_m \\ &= \sqrt{E_S} \sum_{d=1}^D \left( x_d \sum_{n \in \{d\}_D^N} [\mathbf{H}_V]_{m,n} \right) + z_m \end{aligned} \quad (31)$$

where  $[\mathbf{H}_V]_{m,n}$  denotes the  $(m,n)$ -th entry of the virtual channel matrix  $\mathbf{H}_V$ . Hence, the channel equation under virtual angle grouping becomes

$$\mathbf{y} = \sqrt{E_S} \tilde{\mathbf{H}}_V \tilde{\mathbf{x}} + \mathbf{z} \quad (32)$$

where  $\tilde{\mathbf{x}} = (x_1, \dots, x_d)^\top$  and the  $(m,d)$ -th entry of the  $M \times D$  virtual channel matrix  $\tilde{\mathbf{H}}_V$  is given by

$$[\tilde{\mathbf{H}}_V]_{m,d} = \sum_{n \in \{d\}_D^N} [\mathbf{H}_V]_{m,n}. \quad (33)$$

Since the generating code  $\mathcal{G}^D$  occupies spatial virtual angles 1 to  $D$ , the space-time  $D$ -block code  $\mathcal{C}^{(D,N)}$  can be viewed as applying the space-time block code  $\mathcal{G}^D$  on the channel matrix  $\mathbf{H}_V$  induced by virtual angle grouping. The original virtual channel coefficients are partitioned according to modular classes by (33). Codewords can only resolve each modular class rather than each individual element of virtual channel matrix. Since all the coefficients in one modular class are added together, only one level of diversity can be attained although the effective received channel power is increased due to the uncorrelated nature of virtual channel coefficients. It follows that space-time  $D$ -block codes can achieve a maximum of  $D \times M$  level of diversity with  $D$  level of diversity per receive dimension. For a  $K$ -diagonal channel, its nonvanishing elements are confined in a band with width  $D_N(K)$ . Choosing  $D = D_N(K)$ , it is easy to verify that each of the  $D$  modular classes contains at most one nonvanishing element of  $\mathbf{H}_V$ . Hence, space-time  $D$ -block codes achieve full diversity by matching  $D$  with the underlying channel structure. However, when there are more than

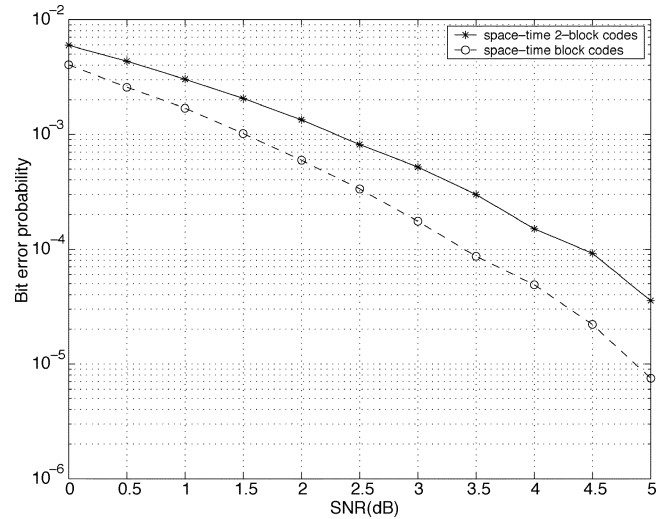


Fig. 7. Bit-error probability of space-time two-block codes and space-time block codes on  $4 \times 4$  fully populated i.i.d. channels. 4QAM is used at every transmit element.

one nonvanishing elements of  $\mathbf{H}_V$  residing in the same class, a diversity loss may occur due to virtual angle grouping.

“Diminishing returns” of diversity are well-known—a few initial gains in diversity significantly enhance system performance while further diversity increments bring marginal gains. In this context, the  $K$ -diagonal model would serve as a useful approximation to i.i.d. channels as well. In Fig. 7, we plot the simulated bit error probability performance of space-time two-block codes (achieving two level of diversity per dimension) and space-time block codes (achieving full diversity) on a fully i.i.d.  $4 \times 4$  virtual channel. The figure demonstrates that  $D = 2$  could bring comparable performance with respect to that of space-time block codes due to diminishing returns of diversity. Furthermore, relatively low  $K$ -diagonal approximations are even more effective for larger number of antennas.

Our discussion shows that space-time  $D$ -block codes could provide a flexible tradeoff between diversity and complexity via virtual angle grouping. Smaller  $D$  could lower decoding delay and complexity, while larger  $D$  could achieve higher diversity. In view of the diminishing diversity returns, the designer may favor smaller  $D$  to reduce delay while still maintaining reasonable performance.

#### V. RATE VERSUS DIVERSITY TRADEOFF

The effective channel in (28) implies that space-time block codes including space-time  $D$ -block codes incur an inherent loss of spatial parallel channels; the original MIMO channel has “collapsed” to a one-dimensional scalar channel though with full diversity. It is well known that diversity offers diminishing improvements in probability of error as the level of diversity grows. Furthermore, the loss in parallel channels incurs a significant hit on system capacity. Hence, a considerable capacity penalty is associated with space-time block codes and the like [12], [20], [22]. The needs for higher diversity and higher rate are conflicting for fixed total number of signal-space dimensions. Spatial multiplexing methods such as BLAST use all available dimensions for rate while space-time block codes use all dimensions for diversity. A judicious tradeoff between rate

and diversity is needed for good performance in practice. In this section, we propose a flexible design framework to facilitate the tradeoff. Our approach is to decompose the original MIMO channel into several lower dimensional MIMO subchannels over which parallel data streams can be transmitted. Intuitively, from a signal-space viewpoint, the framework divides the total dimensions into several subchannels each with certain level of diversity and the number of the subchannels is proportional to the rate supported by the system. Again, the framework is cast in the virtual channel representation which exposes the inherent (uncorrelated) degrees of freedom in the channel. We next explain the framework in detail.

Consider a  $K$ -diagonal virtual channel described in (8). One can partition  $\mathbf{H}_V$  as

$$\mathbf{H}_V = \begin{pmatrix} \mathbf{H}_1 & \mathbf{B}_1 & \mathbf{0} & \mathbf{0} \\ \mathbf{A}_2 & \mathbf{H}_2 & \mathbf{B}_2 & \mathbf{0} \\ \mathbf{0} & \ddots & \ddots & \ddots \\ \mathbf{0} & \mathbf{0} & \mathbf{A}_P & \mathbf{H}_P \end{pmatrix}. \quad (34)$$

If the input and output vectors are partitioned accordingly, a total of  $P$  lower dimensional MIMO subchannels are created. The submatrix  $\mathbf{H}_p$  for  $1 \leq p \leq P$  describes the  $p$ th MIMO subchannel, that is

$$\mathbf{y}_p = \sqrt{E_s} \mathbf{H}_p \mathbf{x}_p + (\mathbf{A}_p \mathbf{x}_{p-1} + \mathbf{B}_p \mathbf{x}_{p+1}) + \mathbf{z}_p \quad (35)$$

where  $\mathbf{x}_p$ ,  $\mathbf{y}_p$  and  $\mathbf{z}_p$  are the input, output and noise of the  $p$ th subchannel, respectively. Since most of the submatrices  $\mathbf{H}_p$  preserve the  $K$ -diagonal structure as the original channel,<sup>2</sup> the original channel has been decomposed into  $P$  parallel  $K$ -diagonal subchannels with lower dimensions, through which a judicious rate-versus-diversity tradeoff can be realized by choosing appropriate dimensions for each subchannel. The diversity of each subchannel is determined by the number of nonvanishing elements in its channel matrix. The larger the dimensions of the subchannel, the more diversity it has. Space-time  $D$ -block codes can be used to achieve full diversity in each subchannel. However, subchannels with larger dimensions (and, hence, higher diversity) could reduce the overall rate. A good decomposition of the original channel needs to take into account both rate and diversity. It is clear that this decomposition idea is quite flexible in that many different rate-versus-diversity combinations can be accommodated.

As shown in (35), the subchannels created by the above decomposition are not independent of each other. Comparing (35) with (8), one could regard the second term in (35) as interference from other subchannels to the  $p$ th subchannel. As demonstrated in our simulations, such interference would, if left untreated, cause an error-floor in performance. Interference cancellation techniques are generally required to improve system performance. To this end, we propose a decision feedback interference cancellation algorithm which is able to effectively reduce the amount of interference among different subchannels. The basic idea is to subtract from the received signal the interference estimated using initial decisions. Then, refined decisions can be obtained from the ‘‘cleaner’’ signal and they, in turn, improve the quality of inference cancellation. The algorithm can operate in several iterations before final decisions are made. Formally we have the following algorithm.

<sup>2</sup>submatrices may have different values of  $K$ .

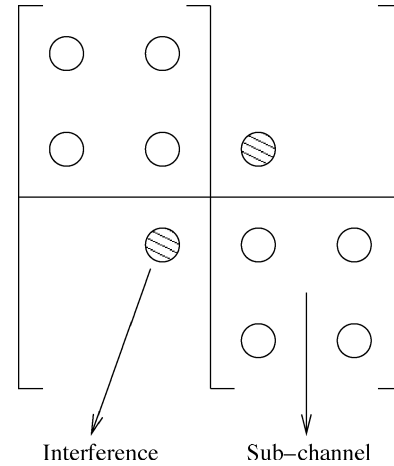


Fig. 8. Schematic illustrating the subchannel decomposition for a 3-diagonal channel with dimension  $4 \times 4$ . The circles in the figure represent nonvanishing elements in the channel matrix. The shadowed circles represent the interference among the two subchannels.

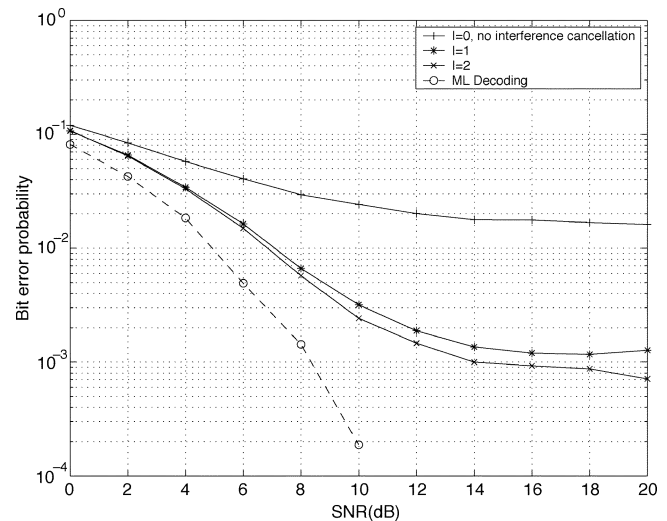


Fig. 9. Performance of the proposed interference cancellation algorithm for a three-diagonal channel with dimension  $4 \times 4$ . Two  $2 \times 2$  subchannels are created from the original channel. 4QAM is used at each transmit element. The number of interactions,  $I$ , varies from 0 (no interference cancellation) to 2.

*Algorithm 1:* Let  $\tilde{\mathbf{H}}_V = \text{diag}(\mathbf{H}_1, \dots, \mathbf{H}_P)$  be the block diagonal matrix formed by taking the block diagonal of  $\mathbf{H}_V$  in (34). Denote by  $I$  the number of iterations.

- 1) Let  $\tilde{\mathbf{y}} = \mathbf{y}$ .
- 2) Decode each subchannel separately to generate a decision for channel input  $\tilde{\mathbf{x}}$ .
- 3) Subtract interference in parallel. The refined received signal  $\tilde{\mathbf{y}}$  is given by

$$\tilde{\mathbf{y}} = \mathbf{y} - \sqrt{E_s} (\mathbf{H}_V - \tilde{\mathbf{H}}_V) \tilde{\mathbf{x}}. \quad (36)$$

- 4) Repeat Step 2 and 3 by  $I$  times.

To illustrate this framework, we apply it to a three-diagonal channel with dimension  $4 \times 4$ . The original  $4 \times 4$  channel is decomposed into two subchannels each with dimension  $2 \times 2$  as shown in Fig. 8. The nonvanishing elements in the three-diagonal channel are represented by small circles in the figure. After the partition, the shadowed circles represent the interference among subchannels. Space-time two-block codes are used

in each subchannel to achieve a diversity order of 4 and a rate of 2 complex symbols per channel is supported. In Fig. 9, we plot the simulated system performance. It can be seen that the interference among subchannels results in an error floor in bit error probability. The proposed interference cancellation algorithm exhibits an impressive performance to combat the interference—one iteration could reduce BER by one order of magnitude although an error floor exists due to residual interference caused by imperfect interference cancellation. The performance of the maximum likelihood (ML) decoding is also included in the figure. It is shown that ML methods can offer a substantial performance improvement over interference cancellation techniques especially in the large SNR regime. However, the complexity of ML methods is exponential with respect to system dimension. The total cardinality of the signal points is 256 for the maximum likelihood decoding in the figure.

## VI. CONCLUSION

We have proposed a framework for space-time block code design for correlated MIMO channels based on the virtual channel representation. The centerpiece of our framework is space-time  $D$ -block codes that are matched to the  $K$ -diagonal virtual channel model. Only the knowledge of the parameter  $K$ , which characterizes channel correlation/diversity in the  $K$ -diagonal model, is assumed at the transmitter. The  $K$ -diagonal model can be motivated by physical scattering consideration and also serves as a useful building block for representing more general channels. The results of this paper demonstrate the utility of the proposed virtual representation framework: 1) it greatly simplifies PEP analysis for correlated channels, 2) space-time  $D$ -block codes can deliver performance comparable to existing block codes but with significantly lower delay and complexity, and 3) the virtual channel representation naturally facilitates the fundamental trade-off between rate and diversity in MIMO channels. We are currently investigating the use of the virtual representation framework in space-time trellis coding, linear dispersion coding, and information theoretic aspects of MIMO channels.

## REFERENCES

- [1] G. J. Foschini, "Layered space-time architecture for wireless communication in a fading environment when using multi-element antennas," *Bell Labs Tech. J.*, vol. 1, no. 2, pp. 41–59, Autumn 1996.
- [2] I. E. Telatar, "Capacity of multi-antenna Gaussian channels," AT&T Bell Labs, Tech. Rep., 1995.
- [3] V. Tarokh, N. Seshadri, and A. R. Calderbank, "Space-time codes for high data rate wireless communication: performance criterion and code construction," *IEEE Trans. Inform. Theory*, vol. 44, pp. 744–765, Mar. 1998.
- [4] A. J. Paulraj and C. B. Papadias, "Space-time processing for wireless communications," *IEEE Signal Processing Mag.*, pp. 49–83, Nov. 1997.
- [5] A. M. Sayeed, "Deconstructing multi-antenna fading channels," *IEEE Trans. Signal Processing*, vol. 50, pp. 2563–2579, Oct. 2002.
- [6] D. Shiu, G. J. Foschini, M. J. Gans, and J. M. Kahn, "Fading correlation and its effect on the capacity of multi-element antenna systems," *IEEE Trans. Commun.*, vol. 48, pp. 502–512, Mar. 2000.
- [7] D. Gesbert, H. Bolcskei, D. Gore, and A. Paulraj, "Outdoor MIMO wireless channels: Models and performance prediction," *IEEE Trans. Commun.*, vol. 50, pp. 1926–1934, Dec. 2002.
- [8] M. O. Damen, A. Abdi, and M. Kaveh, "On the effect of correlated fading on several space-time coding and detection schemes," in *Proc. IEEE Vehicular Technology Conf.*, Atlantic City, NJ, Oct. 2001.

- [9] M. Uysal and C. N. Georghiadis, "Effect of spatial fading correlation on performance of space-time codes," *Electron. Lett.*, vol. 37, pp. 181–183, Feb. 2001.
- [10] S. Siwamogsatham and M. P. Fitz, "Robust space-time coding for correlated Rayleigh fading channels," in *Proc. 38th Allerton Conf. Communications, Control, Computing*, Monticello, IL, Oct. 2000.
- [11] V. Tarokh, H. Jafarkhani, and A. R. Calderbank, "Space-time block codes from orthogonal designs," *IEEE Trans. Inform. Theory*, vol. 45, pp. 1456–1467, July 1999.
- [12] S. Sandhu and A. Paulraj, "Space-time block codes: A capacity perspective," *IEEE Comm. Lett.*, vol. 4, pp. 384–386, Dec. 2000.
- [13] B. Hassibi and B. M. Hochwald, "High-rate codes that are linear in space and time," *IEEE Trans. Inform. Theory*, vol. 48, pp. 1804–1824, July 2002.
- [14] V. Tarokh, A. Naguib, N. Seshadri, and A. R. Calderbank, "Combined array processing and space-time coding," *IEEE Trans. Inform. Theory*, vol. 45, pp. 1121–1128, May 1999.
- [15] R. A. Horn and C. R. Johnson, *Matrix Analysis*. New York: Cambridge Univ. Press, 1988.
- [16] J. Fuhl, A. F. Molisch, and E. Bonek, "Unified channel model for mobile radio systems with smart antennas," *IEEE Proc. Radar, Sonar Navig.*, vol. 145, pp. 32–41, Feb. 1998.
- [17] L. H. Ozarow, S. Shamai, and A. D. Wyner, "Information theoretic considerations for cellular mobile radio," *IEEE Trans. Veh. Technol.*, vol. 43, pp. 359–378, May 1994.
- [18] S. Siwamogsatham, M. P. Fitz, and J. H. Grimm, "A new view of performance analysis of transmit diversity schemes in correlated Rayleigh fading," *IEEE Trans. Inform. Theory*, vol. 48, pp. 950–956, Apr. 2002.
- [19] A. V. Geramita and J. Seberry, *Orthogonal Designs, Quadratic Forms and Hadamard Matrices*, ser. Lecture Notes in Pure and Applied Mathematics. New York: Marcel Dekker, 1979, vol. 43.
- [20] K. Liu and A. M. Sayeed, "Layered transmit diversity," in *Proc. Int. Conf. Acoustics, Speech and Signal Processing*, Orlando, FL, May 2002, pp. III-2421–III-2424.
- [21] S. M. Alamouti, "A simple transmit diversity technique for wireless communications," *IEEE J. Select. Areas Commun.*, vol. 16, pp. 1451–1458, Oct. 1998.
- [22] K. Liu and A. M. Sayeed, "Space-time multiplexing for multi-antenna channels," in *Proc. IEEE Int. Symp. Information Theory*, Lausanne, Switzerland, July 2002, p. 222.
- [23] G. L. Stuber, *Principles of Mobile Communication*, 2nd ed. Norwell, MA: Kluwer, 2001.



**Ke Liu** (S'99) received the B.S. degree in electrical engineering from Tsinghua University, Beijing, China, in 1999, and the M.S. degree in electrical engineering and the M.A. in mathematics from University of Wisconsin-Madison, in 2001 and 2002, respectively, where he is currently working toward the Ph.D. degree in electrical engineering.

His research interests include information theory, wireless communications, wireless ad hoc networks, and statistical signal processing.



**Akbar M. Sayeed** (S'89–M'97–SM'02) received the B.S. degree from the University of Wisconsin-Madison in 1991, and the M.S. and Ph.D. degrees in electrical and computer engineering from the University of Illinois at Urbana-Champaign, in 1993 and in 1996, respectively.

While at the University of Illinois, he was a Research Assistant in the Coordinated Science Laboratory and was also the Schlumberger Fellow in signal processing from 1992 to 1995. From 1996 to 1997, he was a Postdoctoral Fellow at Rice University, Houston, TX. Since August 1997, he has been with the University of Wisconsin-Madison, where he is currently an Assistant Professor in electrical and computer engineering. His research interests include wireless communications, sensor networks, statistical signal processing, wavelets, and time-frequency analysis.

Dr. Sayeed served as an Associate Editor for the IEEE SIGNAL PROCESSING LETTERS from 1999 to 2002. He received the NSF CAREER Award in 1999 and the ONR Young Investigator Award in 2001.